Energy & Environmental Science
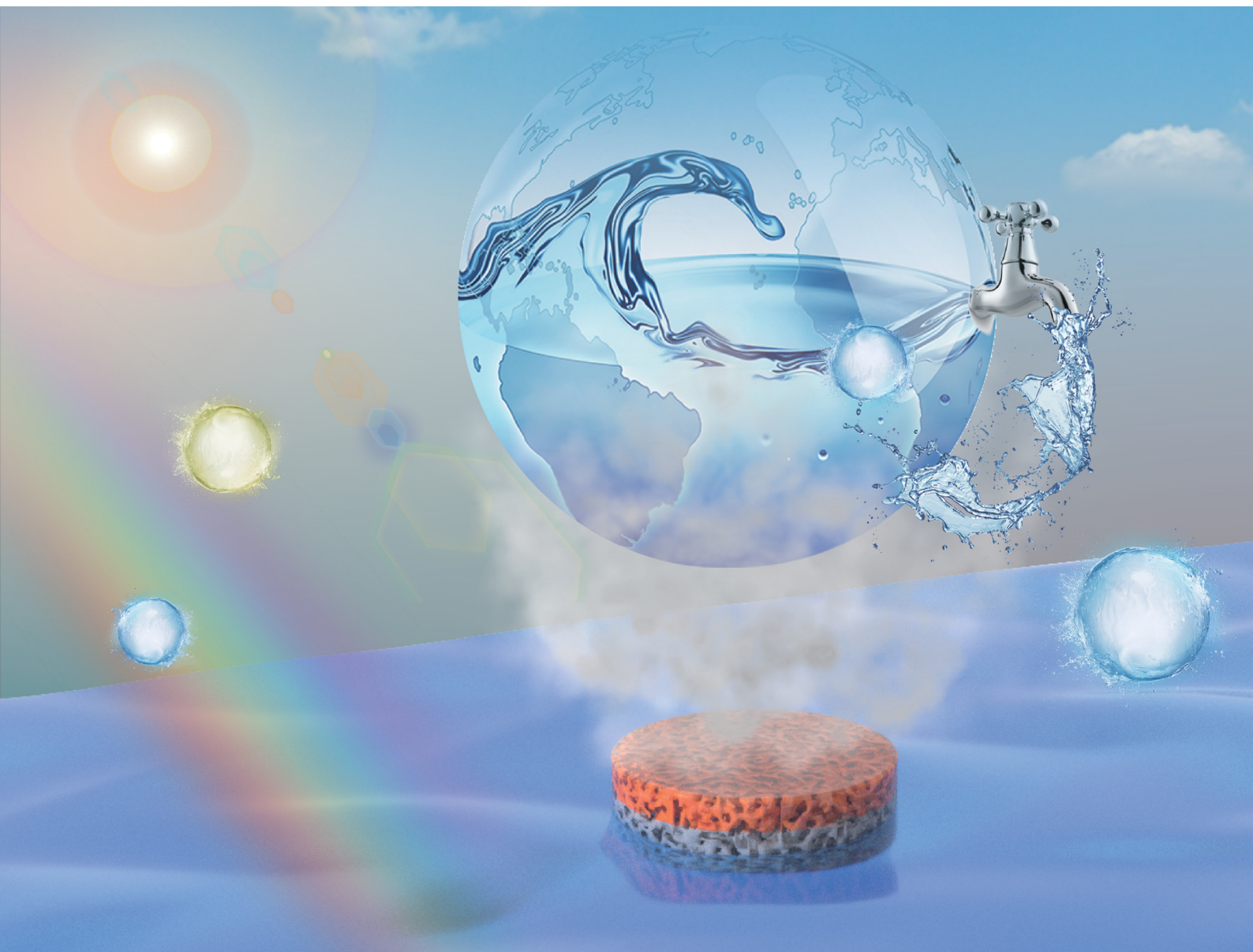
PERSPECTIVE
Haolan Xu, Qiang Fu *et al.*
Updated perspective on solar steam generation application

Check for updates

Updated perspective on solar steam generation application

Casey Onggowarsito, [a] Shudi Mao, [a] Xin Stella Zhang, [a] An Feng, [a] Haolan Xu *[b] and Qiang Fu *[a]

A low cost, highly flexible and environmentally friendly water generation method known as interfacial solar steam generation (SSG) has recently been popularized by many researchers due to the continuously increasing water demand and widening wealth gap around the world. In this perspective, factors determining SSG performance are gathered and highlighted in two different categories, heat and water management. This perspective also identifies challenges that hinder the practical applications of SSG, such as the lack of a standardized energy conversion efficiency calculation, understanding the water evaporation mechanism, understanding the heat flow from the ambient environment to the three-dimensional SSG, focusing solely on the evaporation rate (R_v) while ignoring vapor collection efficiency, and the relatively single function that is unable to cope with complex external environments (*i.e.*, anti-fouling). This perspective also discusses current trends in multifunctional applications of SSGs, such as antimicrobial and energy generation properties, and provides insights into future research prospects for SSGs.

Broader context

Due to industrial and agricultural development, growing population and climate change on the environment, our demand for water supply is constantly increasing. To alleviate this challenge, a promising and portable water generation method known as interfacial solar steam generation (SSG) has been proposed due to its low-cost, ease of operation and environmental friendliness. Over the last few years, numerous studies have demonstrated important factors that contribute to improving water production performance and efficiency. This perspective outlines the unaddressed issues in this domain, discusses SSG design principles, and highlights future research prospects and the directions for practical applications of SSG, thereby providing a feasible pathway for alleviating water stress in arid regions.

[a] Centre for Technology in Water and Wastewater, School of Civil and Environmental Engineering, University of Technology Sydney, Ultimo, New South Wales 2007, Australia. E-mail: qiang.fu@uts.edu.au

[b] Future Industries Institute, University of South Australia, Mawson Lakes Campus, South Australia 5095, Australia. E-mail: haolan.xu@unisa.edu.au

Casey Onggowarsito received his BS degree at the University of New South Wales. He is currently working towards his PhD degree at the University of Technology Sydney under the supervision of Dr Qiang Fu. His current research focuses on synthesizing hydrogel-based materials for water purification.
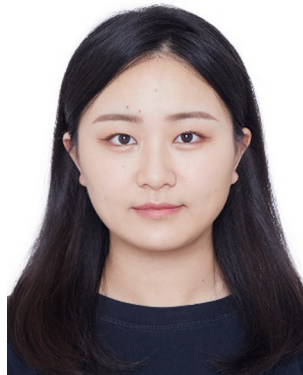
Casey Onggowarsito

Shudi Mao received her BEng from Huazhong University of Science and Technology in 2017 and her MS from East China Normal University in 2020. She is currently pursuing her PhD at the University of Technology Sydney, with research interests in advanced polymeric materials design and synthesis for water treatment.

Shudi Mao

1. Introduction

Water demand has continuously grown at a fast rate of 1% every year due to industrial/manufacturing, agricultural, domestic activities, and accumulating wastewater.[1–3] However, current desalination plants generally require huge initial investment and consume a lot of energy to operate, so they are not yet practical for poor, arid regions. In order to keep up with this water demand, there has been a reasonably high amount of attention in interfacial evaporation *via* solar energy known as solar steam generation (SSG) due to its cost-effectiveness and environmentally friendly method,[4] bringing an alternative solution in supplying our current water demand.[5–7]

The basic mechanism of an SSG system relies on sunlight exposure or solar irradiation to drive an active and continuous water evaporation. This is achieved by capturing the exposed solar energy and converting it into thermal energy *via* a photothermal material (PTM).[8] However, there are common challenges that needed to be addressed to generate an efficient water evaporation. These challenges include the loss of thermal energy towards bulk water and surrounding and having a broader spectral light absorption capability in order to harvest majority of the solar energy. Besides SSG heat management aspect, current interfacial SSG system also focuses on water management strategy. Common solution that many recent studies have provided is to utilize hydrophilic absorbent for balanced water replenishment and evaporation, generating an efficient water transport system. Despite this, there are still challenges that are unaddressed in this aspect such as understanding water molecules interaction within different hydrophilic materials, water evaporation mechanism, and material's parameters that affects water transport efficiency.[9] Moreover, filtration competency of SSG is crucial in order for SSG system to be considered as a greener alternative in freshwater production. There have been many studies that focused on desalination and organic compound filtration. However, there are limited number of studies that discussed the importance of microbial filtration.[10–13]

In addition to water evaporation performance, another aspect that are rarely discussed in previous studies is efficient water collection. This is important in calculating freshwater yield for average water consumption to potentially replace current water production systems. Apart from SSG practical aspect, there has been some theoretical inconsistency[14] regarding SSG conversion

Xin Stella Zhang received her BEng from Shenyang University of Chemical Technology in 2014 and her MEng in Chemical and Biomolecular Engineering from The University of Sydney in 2018. She is currently working towards her PhD degree at the University of Technology Sydney. Her research focuses on boron-based nanomaterials, polymer hydrogels, desalination and water treatment.

Xin Stella Zhang

An Feng is a current PhD student focusing on next generation polymeric atmospheric water harvesting materials at the University of Technology Sydney. He completed his BE in Chemical Engineering and Technology from Chongqing University in 2017, and MEng in Chemical Engineering from The University of Melbourne in 2020.

An Feng

Dr Haolan Xu is a Professor at Future Industries Institute, the University of South Australia. He obtained his PhD degree at Shanghai Institute of Ceramics, Chinese Academy of Sciences in 2008. Then he worked at Max Planck Institute of Colloids and Interfaces as an Alexander von Humboldt Postdoctoral Fellow. He joined The University of South Australia in January 2011. His research interests include colloid and interface physical chemistry, catalysis, solar-thermal energy conversion and applications.

Haolan Xu

Dr Qiang Fu is an Associate Professor at the Centre for Technology in Water and Wastewater (CTWW), University of Technology Sydney. He obtained his PhD degree in Polymer Chemistry and Physicals from Fudan University in 2009 before working as a postdoctoral fellow at the University of Melbourne. He joined the University of Technology Sydney in October 2019. The research interests in Dr Fu's group include solar steam generation, 2D materials, MOFs, functional polymer materials, and membrane nanotechnology for energy and environmental applications.

Qiang Fu

efficiency calculation and surface area evaporation throughout recent studies. This resulted in many inaccurate comparison studies, with some SSG studies demonstrating efficiencies exceeding 100%.

In this contribution, we first identified research challenges in this domain, such as not having a standardization energy conversion efficiency calculation, water transport mechanism, and the misunderstanding of calculated projected areas for determining water evaporation rate (R_v). These problems are crucial to be understand and resolve in order to further understand and improve future SSG systems as will be further discuss. Furthermore, we provide new perspective of heat and water management, as well as multi-functioning SSG is discussed and highlighted, summarizing the important factors in designing SSG system and broadening future application of SSG (Fig. 1).

2. Heat management

Heat generation has been an important factor in SSG as high temperature promotes faster water evaporation.[15,16] Many previous SSG systems have pursued heat generation performance through introducing different types of PTM with potentially a short bandgap for a broader light absorption.[10] Besides this, a recent study has highlighted another important aspect of developing a PTM with high joint density of states (JDOS). The existence of high JDOS allows for high population of hot electrons and holes, promoting higher photoexcitation, broadening the wavelength range for light absorption, as well as a faster relaxation process of the photoexcited carriers.[17] In addition, this segment highlights the challenges in optimizing the SSG heat conversion efficiency in order to minimize any energy loss produced. Furthermore, this perspective revises previously known while introduces new factors that may play the role in improving SSG heat management strategy (Fig. 2).

2.1. Surface roughness

The commonly produced frozen-dried gel-based polymer SSGs are well known for their increase in surface roughness which significantly affects its light absorption property. This effect is caused by the multiple light reflection and scattering throughout the surface (Fig. 2i).[18–20] One study reported that the utilization of modified nickel nanoparticles was able to adjust the film's surface structure by exposing each film to specific magnetic field strength. As a result, an increase in surface roughness would lead to an increased photothermal efficiency (or a decrease in energy loss) and hence R_v.[21] Interestingly, tuning the surface roughness can also alternate the surface hydrophilicity to optimized SSG performance.[20,22]

2.2. Heat isolation

Solar-thermal energy generated by PTM is known to be loss to its surrounding environment *via* conduction, convection, and irradiation due to the higher evaporation surface temperature relative to the surrounding temperature. For typical 2D evaporators, a common issue faced in developing SSG is the huge thermal loss towards the bulk water.[10,21,23] In order to minimize this energy loss, heat isolation is one of the important factors in designing interfacial SSG systems. Besides using a low thermal conductive material as a water absorbing substrate (Fig. 2ii),[20,24] strategy such as Janus membrane is a common method that has been thoroughly studied to achieve SSG heat isolation. Furthermore, Janus membrane also displays salt-resistance property.[25–27] This can be seen in a recent example of a 3D cone shaped Janus evaporator that was able to generate a stable performance of approximately 1.650 kg m^{-2} h^{-1} of brine water evaporation with no salt-fouling.[28] Other strategies include using foam platform[29,30] or attaching cellulose filter paper onto the SSG hydrogel to increase the temperature difference between the surface temperature, heated hydrogel and the bulk water.[31] For 3D evaporators, they may be able to extract energy from the bulk water to enhance solar evaporation.[32] In this case, highly thermal conductive materials instead of thermal insulation ones should be utilized.

2.3. Vapor flow

A recent study has brought a new aspect in identifying the correlation between the SSG surface area with its water evaporation performance. The study found that an increase in evaporator surface size leads to a decrease in evaporation rate.
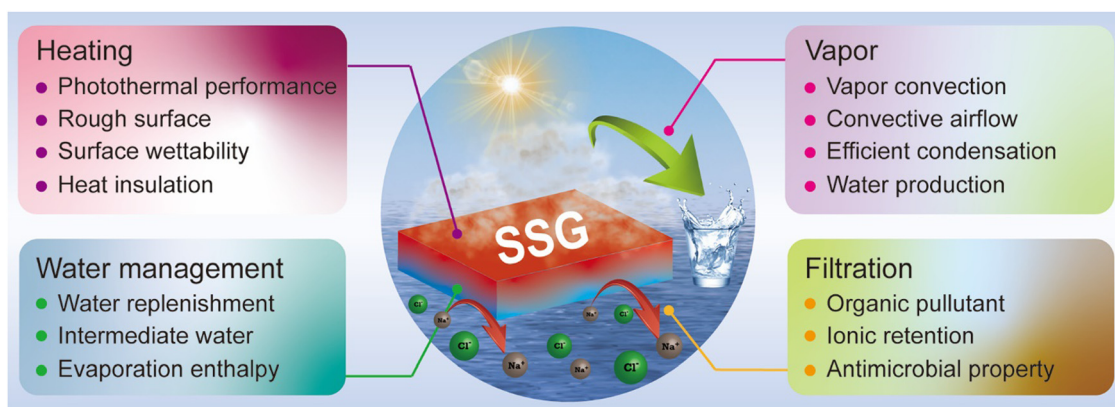

Fig. 1 Schematic diagram of solar steam generator design and its desalination process.
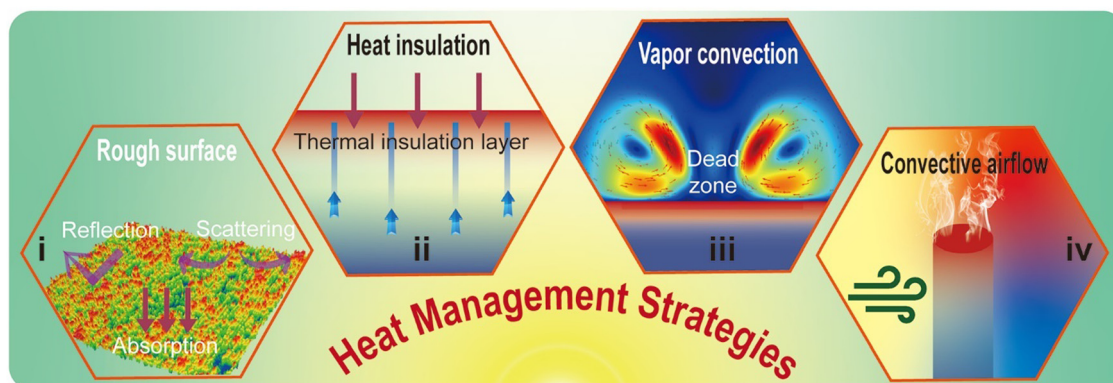
2090 | *Energy Environ. Sci.*, 2024, **17**, 2088–2099

This journal is © The Royal Society of Chemistry 2024

Fig. 2 Heat management strategies involving (i) material's surface roughness, (ii) heat isolation to avoid any energy loss, (iii) material's surface area affecting vapor flow for efficient evaporation, and (iv) the use of external convection airflow.

This phenomenon can be attributed to the dead evaporation zone (Fig. 2iii) where there is no convection flow covered at the center area of the big evaporative surface to remove the accumulated vapor generated by water evaporation. This finding further demonstrated that by removing an optimized area in the center of the evaporation surface allowed the both water evaporation rate and vapor output to increase.[33]

2.4. Convective airflow

Other studies have also observed the advantage of introducing an external convective airflow (Fig. 2iv) to their system *via* artificial or natural wind, as it allows the SSG system to reduce the surrounding vapor pressure or humidity produced by the water evaporation, as well as lowering the surface temperature which leads to reduced energy loss *via* radiation and convection, or in some case even allow the evaporation surface harvest extra energy from the surrounding air.[34–37] One study managed to demonstrate a hydrogel with exposure of external air can generate $10\times$ greater water evaporation performance at an optimal airflow speed of 0.75 m s^{-1} at 25 °C compared to the enclosed hydrogel. Additionally, this observation indicated that a high airflow temperature caused by the excess heat produced by solar energy can potentially reduce the evaporation efficiency due to the weakening of the heat transfer from the PTM layer to the feed water, causing excess heat loss to

the feed water.[38] Additionally, another study was able to design an updraft airflow using temperature gradient. Inspired by a flower like structure, the solar absorbing bottom plate covered by carbon tape generates heat while the carbon-coated PVA upper layer was set on an angle and acts as an evaporator. The temperature difference between the bottom and upper layer generates an updraft airflow which helps to increase the water evaporation efficiency.[39]

3. Water management

Besides just having an optimized heat management system, water management also plays a crucial role in generation fast water evaporation (Fig. 3). A recent study highlighted the fact that water evaporation rate does not directly correlates towards SSG energy conversion efficiency, rather its low evaporation enthalpy and fast rehydration rate instead. Therefore, this study conveyed the importance of having an efficient water management system such as increasing intermediate water content and maximizing water transport.[12]

3.1. Water transport

Recent studies have addressed some factors which may or may not affect the water transport kinetic of a SSG system (Fig. 3i).
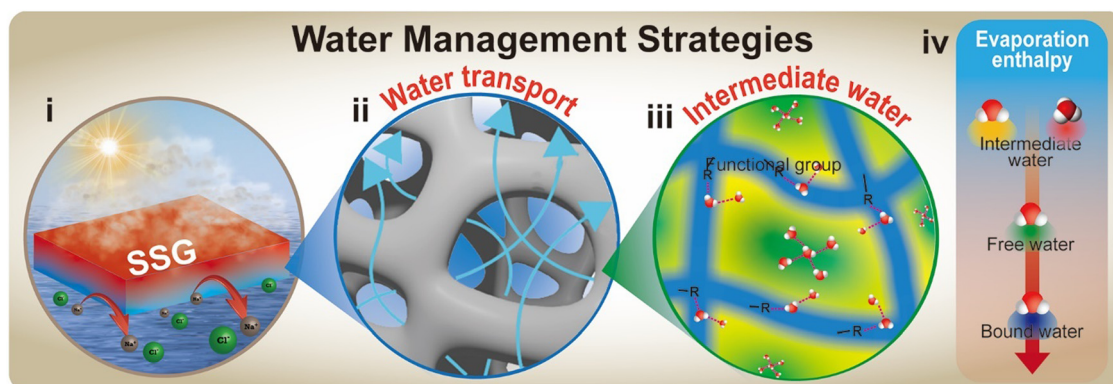

Fig. 3 Schematic diagram of water management strategies.

This journal is © The Royal Society of Chemistry 2024

Energy Environ. Sci., 2024, **17**, 2088–2099 | **2091**

Crosslinking density are known to affect the mechanical properties of a polymer network.[40] However, factors such as crosslinking density and high porosity of a polymer matrix are also commonly addressed in relation towards water transport.

For example, one study failed to discover a correlation between the difference in crosslinking density and the pore size generated, through utilizing crosslinked MXene-based aerogel films (MAFs) *via* ferrous ions. Despite this, they found that there is an optimum crosslinking level of MXene/FeCl$_2$ mass ratio to generate the highest water evaporation performance (1.67 kg m^{-2} h^{-1}) compared to other mass ratios (Fig. 3ii).[19] Another study observed a similar effect of water transport in regard to the degree of crosslinking. This phenomenon was showed through glutaraldehyde crosslinked PVA hydrogels at different freezing time and further proposed that the larger pores can be generated by disrupting PVA sequence which therefore weakens the ice recrystallization inhibition activity. However, PVA-0h where it was frozen instantly demonstrated that it has a significantly higher water absorptivity and faster half saturation time compared to PVA-2h which was left reaction at R.T. for 2 hours. This result suggests that narrower channels provide a stronger capillary action compared to larger pores.[41] On the contrary, a previously mentioned study demonstrated that the water transport rate and half saturation time of IPHs increases relative to its increasing pore size.[42] Additionally, another previously mentioned study demonstrated that the increased pore size of cryogels were able to provide a faster water transport rate compared to hydrogels with smaller pore size.[12]

In another case, a PANI-PA SSG membrane porosity showed a negligible corresponding affect towards the SSG water evaporation rate.[43] It is theorized that this is due to the water kinetic diameter being smaller than the mean pore size of the membrane itself. This therefore does not allow the pores to hinder the water molecules passing through the membrane. In all, there is still a knowledge gap in knowing whether crosslinking and pore size could potentially affect SSG water transport kinetic.

3.2. Intermediate water content

Water molecules are known to undertake three different bonding phases when bounded on an SSG substrate. These bonding phases are categorized as bound, free/bulk, and intermediate water. Bound water contains a strong interaction with the substrate's hydrophilic functional groups, whereas free water has negligible interaction. In between these phases is the intermediate water, where it has a weaker hydrogen bond with either the polymer's network or the surrounding water molecules.[44–46]

A recent study highlighted the importance of water dissociation towards introducing the mechanism of intermediate water (Fig. 3iii) to reduce the water evaporation enthalpy. Water dissociation can occur spontaneously at finite temperatures due to its low energy barrier. A recent novel λ-Ti$_3$O$_5$ SSG with a U-shaped structure surface was able to promote intermediate water *via* water dissociation. This is because water molecules obtained from the air was chemisorbed onto this U-shaped groove and was able to hydroxylate with other water molecules

forming physisorption and water dissociation, shown *via ab initio* molecular dynamics (AIMD). As a result, some dissociated H atoms tend to bind with other water molecules forming intermediate H$_3$O* units. These units are metastable and therefore contain frequent proton exchanges between the physisorbed and neighboring water molecules. This phenomenon then causes the back-and-forth transfer between H$_3$O* and H$_2$O, allowing for water evaporation *via* small clusters. Therefore, less energy is required to break the short H$_3$O* hydrogen bonds leading to easy water evaporation.[17]

The increase in intermediate water can be associated to the hydrophilicity of the material. One example study reported that the increase of oxygenated functional groups provided by the GO (PTM) can increase the hydrophilicity of the hydrogel/reduced graphene oxide (rGO) system which allows the hydrogel to form weak hydrogen bonding with the water molecules, and therefore resulting in more intermediate water content.[47] This was demonstrated by the intermediate water to free water ratio content characterized by Raman spectroscopy. The OH stretching modes of water molecules can be determined and categorized between 3200–3600 cm^{-1}. The strong four hydrogen bond water molecules can be found with peaks at 3233 and 3401 cm^{-1}, indicating free water ratio. The weakly broken hydrogen bond water molecules can be found with peaks at 3514 and 3630 cm^{-1}, indicating intermediate water ratio.[48]

Similarly, another study demonstrated that an increased intermediate water is associated with the increase in hydrophilic chitosan ratio within the highly hydratable light-absorbing hydrogel (h-LAH) SSG system.[49] Besides increasing material's hydrophilicity and surface area, intermediate water generation can also be affected by the pore size of the SSG substrate. One study found a correlation between the decreasing interconnected porous hydrogels (IPHs) pore size *via* polymethyl methacrylate (PMMA) particles as a template, promotes a higher intermediate water generation, decreasing its evaporation enthalpy generation (Fig. 3iv).[42]

4. Versatile SSG system

Besides optimizing water production performance, recent studies have focused on filtering organic solvents and desalination performance of seawater through different methods such as photocatalysis (Fig. 4ii), active salt diffusion, electrostatic "Donnan" repulsion (Fig. 4), hydrophilic/hydrophobic Janus membrane, and salt deposition through Marangoni effect.[10] Photocatalysis is a common method in degrading organic compounds by oxidization *via* UV light absorption. For example, a recent carbon foam/TiO$_2$ is able to degrade MB dye (87% degradation) due to TiO$_2$ generation of e$^-$ and h$^+$ *via* UV light absorption as demonstrated by the UV-VIS absorption spectra.[50] Moreover, a common and simple active salt diffusion can be found in many superhydrophilic SSG such as a recently developed self-floating superhydrophilic porous carbon foam (SPCF). SPCF demonstrated excellent its salt-resistant property as it was able to show no salt-accumulation at the evaporator

surface for 8 hours when placed on a 3.5 wt% NaCl saline water. This is because of its efficient and fast water transport *via* its internal microstructure pore that allows the saline water feed to replenish and diffuse excess salt.[51] Additionally, a novel SSG design containing the charges also has excellent salt resistance due to electrostatic repulsion between salt ions and the charges on the SSG material, a phenomenon known as the Donnan effect. As demonstrated by the recent study on PPy-coated porous ionic polymer (PIP) network, which contains cationic groups capable of repelling most salt ions such as K^+, Ca^{2+}, Na^+, and Mg^{2+}, the stable evaporation performance over 6 hours and the reduction in salt ion concentration provide evidence of their effectiveness.[52] Besides this, the previously mentioned 3D cone Janus membrane also able to show its excellent salt-resistant property by having stable water evaporation performance with no salt accumulation on its surface. This is because Janus membrane's hydrophilic/hydrophobic duality layer can selectively allow saltwater to enter. By having a hydrophobic evaporator layer, saltwater cannot enter and therefore accumulate to inhibit the solar-thermal performance of the membrane.[28] Lastly, some SSG studies utilized salt-redirecting *via* Marangoni effect to reject and harvest excess salts. Marangoni/thermo-capillary effect is the flow of liquid caused by the change of liquid surface tension *via* temperature gradient. SSG design such as a recent millineedle hydrogel was able to demonstrate this effect. The temperature difference within the millineedle array surface allows for saltwater to travel to the tip of the needle. At the tip of the needle, the saltwater will evaporate and leave salts to accumulate. These accumulated salts can then be collected and harvested, while water evaporation performance stays unperturbed.[53]

In all, there have been many studies to support future potential desalination, salt-harvesting, and organic pollutants filtration application. Despite this, researchers have also started to focus on the elimination of microbial content which can be found in wastewater or any unfiltered water source. Furthermore, there has been an increasing number of studies to promote alternative energy generation.

4.1.   Anti-microbial

Recent trend in microbial filtration (Fig. 4i) plays an important role in wastewater treatment (Fig. 4iii) application to avoid any potential future health hazards as well as bacterial fouling challenges developed in the SSG system.[31,54] There have been many suggested strategies developed in having anti-microbial property such as oxidation *via* reactive oxygen species (ROS) generation. In an anti-bacterial hydrogel study, ROS were created by the catechol group of the hydrogel chitosan network and accelerated by the quinone modified activated carbon when reacted with oxygen to form quinone groups. As a result, the hydrogel demonstrated > 99% various bacterial (*B. subtilis*, *E. coli*, *P. aeruginosa*) elimination.[55] Another study reported a rGO/agar-agar-based hydrogel whose anti-bacterial/fouling property comes from its surface coated $TaTe_2$ quantum dots (QDs). The incorporated tellurium QDs have strong affinity to DNA sulfur proteins, leading to enhanced permeation of the bacterial membrane and elimination, up to 96.49% and 97.58% for *S. aureus* and *E. coli*, respectively.[31] There are studies in which metallic nanoparticles[56] have been incorporated into SSG material to obtain antimicrobial property through sustained leaching of ions.[57,58]

4.2.   Energy generation

Energy generation/conversion is another multi-functional application that recently has been proposed besides water generation/filtration. Various methods such as hydrovoltaic/electrokinetic, photovoltaic, salinity gradient, piezoelectric and the commonly used Seebeck effect (Fig. 4iv) have been used in electrical energy generation.[24,29,59,60] For example, one study managed to demonstrate the Seebeck effect *via* a 3D
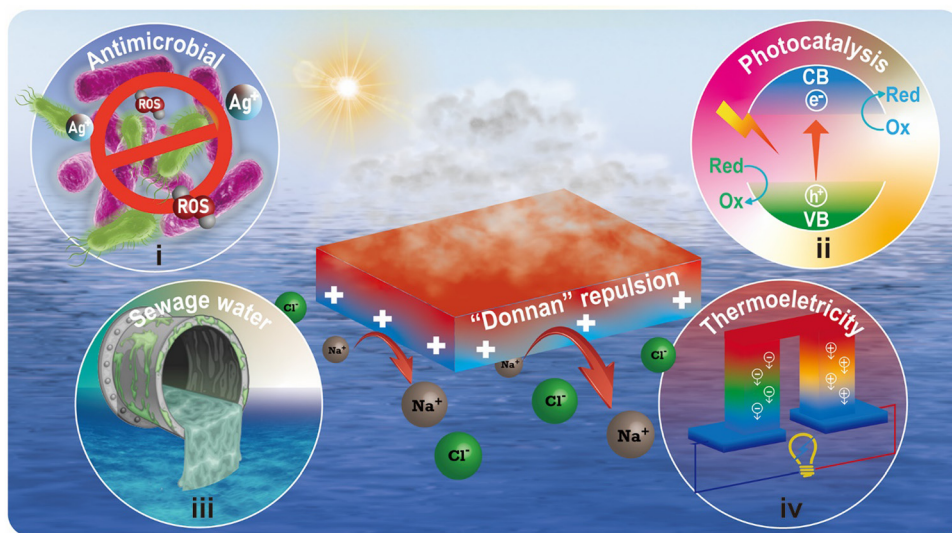

Fig. 4   Schematic diagram of SSG salt-rejection property *via* Donnan repulsion effect, (i) anti-microbial filtration, and (ii) organic compounds photocatalysis degradation for (iii) sewage/wastewater treatment, in addition to (iv) electrical energy generation *via* Seebeck effect.

xerogel foam. The setup includes a thermoelectric (TE) module that was placed in between the xerogel evaporator and thermostatic platform. During solar evaporation, the temperature gradient collected by the TE module between the evaporator converted solar-heat and surrounding low-grade temperature leads to a generated voltage difference. Therefore, the generated temperature gradient from the evaporator allows for electrical energy conversion.[24] Additionally, an aerogel system study was able generate an electrical energy through electric double-layer (EDL) and capillary-driven electrokinetic effect. The capillary effect of fluid passing through the aerogel structure containing negatively charged cellulose nanofibrils (CNFs) layer resulted in salinity gradient. As a result, the buildup EDL leads to the adsorption of positively charge ions, narrowing the channels. This then cause to produce a relatively fast flow rate, followed by the repulsion of negative ions which leads to slower flow rate. The pressure difference from the polarizing flow rate causes voltage difference to be generated.[61,62]

5. Major challenges and prospects

Despite the recent achievements as discussed in the previous section, there are still many future SSG prospects that are needed to be outline in order to further improve SSG system development.

5.1. Theory

Previous studies have shown that the continues water evaporation of SSG is achieved through the photothermal conversion of light to heat produced by PTM material.[48,63,64] A recent comment made has thoroughly discussed the different potential factors which can affect the SSG performance and conversion efficiency consistency. These ranges from the *in situ* experimental setup and conditions, light exposure specifications, and enthalpy calculation.[65] SSG conversion efficiency is commonly calculated by the amount of energy used for water evaporation over the exposed irradiation power. This can be expressed as in eqn (1).

$$\eta = \frac{\dot{m}(C_\mathrm{p}\Delta T + \Delta H_\mathrm{vap})}{c_\mathrm{opt}IA\Delta t} \tag{1}$$

where η is conversion efficiency, $\dot{m}$ is the water evaporation rate, C_p is the specific heat capacity of water (4.18 kJ kg^{-1} K^{-1}), ΔT is the liquid temperature change, ΔH_vap is the vapor latent enthalpy, c_opt is the optical concentration, I is the solar irradiation energy, A is the material's exposed surface area and Δt is the evaporation time.[48,65–67]

In regard to enthalpy, we need to consider the two enthalpy components in determining the SSG efficiency as water transition to vapor. The two enthalpy components consist of sensible heat ($\dot{m}C_\mathrm{p}\Delta T$) and latent heat ($\dot{m}\Delta H_\mathrm{vap}$), which are the energy required to heat up the bulk water to vapor and the energy to change from liquid to vapor phase respectively. In this perspective, we identified that most of current reports neglect the importance of accurate ΔH_vap values for latent heat

determination in the conversion efficiency calculation. This could lead to an inaccurate/inconsistent efficiency measurement and performance comparison between different SSG studies. For example, the constant ΔH_vap value of 2257 kJ kg^{-1} water evaporation enthalpy at 100 °C is commonly used in many SSG studies,[4,63,68] which leads to an overestimation of SSG efficiency (η). With that said, some studies have used a more accurate approximation derived from the Clausius–Clapeyron equation,[69–72] with a maximum error of 0.02% compared to the Smithsonian ΔH_vap values.

$$\Delta H_\mathrm{vap} = 1.91846 \times 10^6 \{T/(T - 33.91)\}^2 \text{ J kg}^{-1} \tag{2}$$

where T is the vapor temperature.[73]

Despite this, the later one may still not be accurate in calculating η due to intermediate water generation when undergoing water evaporation. Many previous studies have demonstrated that the increase in intermediate water content could cause the reduction in ΔH_vap value.[10,64,74] In general, hydrogel-based SSGs with a high intermediate water contents that can be confirmed by Raman Spectra will display lower ΔH_vap based on DSC result.

As shown in eqn (1), the indirect relationship between ΔH_vap and water evaporation rate ($\dot{m}$) highlights the importance of ΔH_vap reduction in order to increase $\dot{m}$ and η. In theory, by having ΔH_vap as 2,257 J g^{-1} at a surface temperature of 100 °C, as well as including the efficiency theoretical limit of 100% light-to-vapour energy conversion efficiency, the maximum $\dot{m}$ should be approximately 1.595 kg m^{-2} h^{-1}. One study reassured this point by demonstrating that by having ΔH_vap as 2257 J g^{-1} violates the energy conservation law due to η resulting as more than 100%. Whereas when ΔH_vap value obtained from DSC measurement, a more reasonable η were obtained.[75] Therefore, majority of research groups have utilized DSC method in obtaining their ΔH_vap.[48,76–80] Having DSC analysis being unavailable, ΔH_vap can also be thermodynamically determined by comparative dark evaporation experiments under controlled temperature and humidity using eqn (3). However, the obtained equivalent ΔH_vap value may end up greater than the DSC determined value. This is because DSC allows full dehydration of SSG material unlike dark static evaporation which may only allow partial evaporation.[48,79]

$$U_\mathrm{in} = \dot{m}_\mathrm{w}\Delta H_\mathrm{w} = \dot{m}_\mathrm{h}\Delta H_\mathrm{vap} \tag{3}$$

where ΔH_w is the bulk water theoretical evaporation enthalpy, ΔH_vap is the evaporator's equivalent evaporation enthalpy, $\dot{m}_\mathrm{w}$ is the mass change of bulk water, and $\dot{m}_\mathrm{h}$ is the mass change of water over the evaporator.

Recently, SSG conversion efficiency can also be found through determining heat loss instead of approximating ΔH_vap value. The solar energy received by the SSG sample can be determined by eqn (4). Moreover, the heat loss caused by conduction, convection, and irradiation can be determined as shown eqn (5). Therefore, the given SSG conversion efficiency can be shown as eqn (6).[10,17]

$$Q_\mathrm{sample} = C_\mathrm{p}m(T_1 - T_2)t \tag{4}$$

$$Q_{loss} = Q_{radiation} + Q_{convection} + Q_{conduction}$$

$$= A\varepsilon\sigma\left(T_1^4 - T_2^4\right)t - Ah(T_1 - T_2)t - A\lambda\frac{\mathrm{d}T}{\mathrm{d}x}t \tag{5}$$

$$\eta = \frac{Q_{sample} + Q_{loss}}{Q_{solar}} \tag{6}$$

where T_1 and T_2 are the surface and surrounding temperature, m is the mass of the SSG sample, t is the exposure time, ε and σ are the emissivity and Steffan–Boltzmann constant, h is the heat transfer coefficient, λ and $\frac{\mathrm{d}T}{\mathrm{d}x}$ are the thermal conductivity and thermal gradient between the sample and water surface.

In summary, the presence of intermediate water (this will be discussed in following paragraph) will cause a significant reduction in ΔH_{vap} for rapid water evaporation due to the weakened hydrogen bonding of the water molecules. Many previous studies have achieved higher performance rate due to the reduced ΔH_{vap} caused by the presence of intermediate water in their systems. It is recommended that the ΔH_{vap} value should be determined through TG-DSC analysis in order to accurately estimate η. In addition, compared to 2D evaporators, identifying ΔH_{vap} of 3D evaporators is more difficult or even impossible due to the presence of various evaporation surfaces with different temperatures and evaporation rates. Therefore, calculation of η become meaningless and is not suggested. The latest theoretical studies have revealed that visible light (λ_{max} = 520 nm) photons can cleave water clusters at the water–vapor interface through the 'photo-molecular effect' (rather than just the photothermal effect). Therefore, researchers should continue to pay attention to the study of the kinetics and thermodynamics of interfacial evaporation in order to be able to better understand the mechanism.

5.2. 2D vs. 3D evaporator

Recent studies have brought many attentions in investigating 3D evaporators due to its high-water evaporation performance compared to 2D evaporators. This is because 3D evaporators are not bound by the theoretical evaporation limit contained in 2D evaporators. This is caused by the larger surface evaporation area that 3D evaporators have over 2D evaporators.[81,82] Moreover, 3D evaporators are able to achieve a lower temperature than the surrounding air during solar steam generation, leading to an evaporative cooling effect. The 3D evaporator can then extract net energy from the environment, which significantly improves water evaporation performance.[28,83,84] This phenomenon can be seen in a transformable rGO coated cellulose sponge (rGO-CS) from a 2D to 3D evaporator. In its 3D phase, the rGO-CS sponge was able to produce a higher water evaporation rate in comparison to its 2D phase under a convective flow. Due to its structure, the 3D sponge allows for elongated heat conduction path which makes its overall surface temperature lower compared to 2D sponge under 1 sun. Moreover, the 3D sponge experienced a much stronger cooling effect brought by the convective flow compared when it is at its 2D phase. As a

result, the 3D sponge structure was able to significantly outperform its 2D counterpart.[32] With that said, developing 3D evaporators is a step in the right direction in realizing future SSG systems.

With this however comes a challenge in determining an appropriate evaporation area to be used in determining evaporation rates since 3D SSG would contain a far larger air/gel interface compared to its 2D predecessor. Previously mentioned comment suggested that the projected area which is the area under collimated illumination is to be used in calculating η.[65] For example, a 3D cylindrical carbonized cattail projected area only takes account of 2 cm diameter exposed top surface. However, the side wall surface area also acts as an evaporator since the cattail is hydrophilic. In effect to this, evaporative cooling is possible due to having the side wall to have a relative lower temperature than the surrounding environment and the top surface. The heat loss generated by the top surface to the surrounding environment can be recollected by the side surface due to thermodynamic. As a result, the increase in cylindrical height will definitely increase the water evaporation rate and efficiency due to the increasing evaporative area. Moreover, the unaccountable side surface area evaporator will produce η to be greater than 100% and exceeds the evaporation theoretical limit.[83]

Another case where projected area may be appropriate to be used in calculating water evaporation rate and efficiency can be seen in the example of a 3D cone evaporator containing a Janus layer of hydrophobic solar absorber inner layer and hydrophilic side evaporative outer layer. This is because the experimental setup involves illuminating the light only on the top solar absorber area. Since the top solar absorber layer is hydrophobic, no water evaporation will take place throughout the projected area. Water evaporation is achieved through the conduction heating of the inner layer to the outer layer of the cone. Furthermore, this study did compare the evaporation rate result between top projected area light exposure with the entire light exposed surface area of the cone. It was found that the entire exposed surface area water evaporation rate is significantly lower in comparison to just top projected area. This can be related back due to the evaporative cooling process as mentioned in the previous example. As a result, η produced by this evaporator is greater than 100%.[28] To avoid this, it is suggested that energy efficiency of 3D evaporators to not be calculated. If it is needed to be calculated, the evaporative cooling area is suggested to be taken accountable in calculating evaporation rate and η. A suggestion perhaps would be including the evaporative cooling rate as dark evaporation rate (unexposed to light) to be subtracted with the light evaporation rate.[65] Moreover, it is recommended that all air/gel interfaces need to be factored into the evaporation rate calculation, since it provides a benchmark for comparison with illuminated evaporation rates.

5.3. Device design

Many previous studies have focused mainly on material development. Therefore, most previous SSG devices such as shown
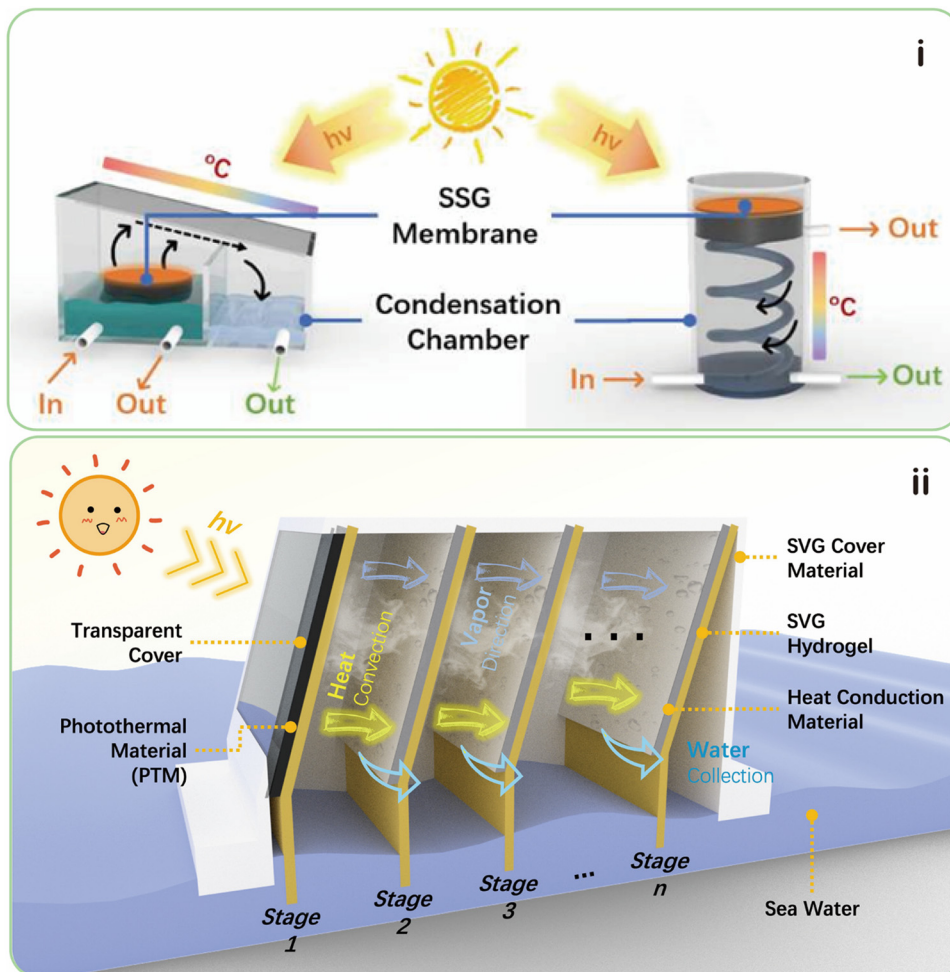
Fig. 5 (i) Conventional *vs.* invert structured SSG device design. (ii) Schematic diagram of multi-stage solar still (MSS) system.

in Fig. 5i are minimalistic, simple, and cost effective. However, these designs may lead to future problems such as the accumulation of water droplets or vapor mist caused by low condensation rates, which can increase light reflection and affect SSG evaporation.[85] In order to eliminate these factors, some studies have introduced a novel invert structured SSG device as shown by the rendering example in Fig. 5i. The concept of invert structured SSG is to constantly cool the hot vapor produced by water evaporation, by using the low temperature of the water feed, thereby increasing the water production rate. One study reported an invert structured SSG system consisting of a solar absorber layer, a hydrophilic water transport layer, and a hydrophobic separator layer contained in a sealed system. The solar absorber layer contains a spectrally selective solar absorber coated on a copper sheet was layered on top of a MoCC-CH$_4$ solar absorber to increase heat conductivity. A hydrophilic nonwoven fabric was layered on the bottom of the solar absorber for continuous unfiltered water transport to be vaporized by the solar absorber. This is then followed by a poly(vinylidene fluoride) (PVDF) hydrophobic membrane layered on the bottom of the hydrophilic layer for vapor-liquid separation. This entire layered system is also supported by a

polystyrene foam platform which acts as a thermal insulation.[67] As a result, a daily freshwater yield of 13.68 kg m^{-2} was achieved using the invert structured SSG under fluctuating solar flux. A similar design named single-stage invert-structured solar water purifier (ISWP) also demonstrated a higher (119%) water production yield compared to a conventional minimalist SSG system.[86] The bottom of the ISWP is a condenser made of a highly thermally conductive material that allows for efficient heat exchange with the environment. Vapor generated in the ISWP system is driven by the vapor pressure gradient to go downward and condensed in the bottom collector, resulting in high vapor collection efficiency.

An alternative to invert structured SSG is to utilize muti-stage design (Fig. 5ii).[87,88] As the name implies, a multi-stage solar still (MSS) contains a PTM with multiple stages of hydrophilic water feed and condenser layer, separated by an air gap or hydrophobic permeable membrane, and a heat sink.[89,90] Despite the similarity of both systems, the invert structured SSG utilizes a low-temperature environment or cooling water to efficiently condense vapor flowing downward into the bottom condenser, greatly improving vapor collection efficiency. While the MSS is designed with a concept that reuses latent heat in

2096 | *Energy Environ. Sci.*, 2024, **17**, 2088–2099

This journal is © The Royal Society of Chemistry 2024

the system, thereby producing fresh water with efficiencies that exceed the thermodynamic limit. For example, a recent CrAlO-based MSS device demonstrated a direct relationship of water production rate and the number of stages. A single stage distiller was able to produce 0.74 kg m^{-2} h^{-1} water production rate under 1 sun. However, an increase to 3 and 6 stages significantly increases its water production rate to 1.28 and 1.84 kg m^{-2} h^{-1} respectively.[91] Despite this, there are still unclear stated parameters within this design such as the number of stages limitation towards water production yield and the length of gap between each stage which could potentially affect water production efficiency.[92]

In all, the design principles for development of next generation SSG should prioritize an effective and efficient vapor collecting system. Hypothetically, a separate active condensation system powered by solar power could potentially serve as an alternative to invert structured SSG systems mentioned, enhancing condensation efficiency for higher water production yields. Besides having an efficient vapor collecting system, a continuous vapor generation may also increase water output yield. From this point of view, maybe in the future we can achieve nighttime water distillation using solar energy to power a certain heating system to accelerate SSG water evaporation.[93,94] Compared to previous SSG devices, this strategy allows the SSG system to continue distilling day and night to produce more freshwater. The downside, however, is the requirement to acquire solar cells and a heating unit. With that said, a new benchmark of water production efficiency can be accounted in L kW^{-1} h^{-1} for this proposed hybrid SSG system as this calculation has been applied in different type of atmospheric water harvesting systems.[95,96]

6. Conclusion

In conclusion, SSG thermal and water management provide fundamental strategies to improve SSG performance and efficiency. Thermal management strategies include reducing vaporization enthalpy, increasing evaporator surface roughness, isolating heat generation, introducing more energy sources, and inducing convectional airflow. Water management strategies include high amount of intermediate water content and ensuring balanced water kinetic transport to the evaporator within the SSG. Despite this, current issues that consist within these strategies are understanding material manipulation to further improve water transport and the misunderstanding of water evaporation areas. Furthermore, the next generation SSGs may have multifunctioning applications beyond water production as demonstrated by recent SSG studies. Future SSG research should focus more on the development and manufacturing of new water production devices, such as high-efficiency steam-water condensation systems, multistage solar still systems and even continuous water production capabilities.

Conflicts of interest

There are no conflicts to declare.

Acknowledgements

References

1 A. Boretti and L. Rosa, *npj Clean Water*, 2019, **2**, 15.
2 G. Mao, H. Hu, X. Liu, J. Crittenden and N. Huang, *Environ. Pollut.*, 2021, **275**, 115785.
3 W.-K. Ho, J. C.-F. Law, T. Zhang and K. S.-Y. Leung, *Water Res.*, 2020, **187**, 116419.
4 X. Zhang, T. Li, W. Liao, D. Chen, Z. Deng, X. Liu and B. Shang, *Nanoscale*, 2022, **14**, 7913–7918.
5 S. Guo, Y. Zhang and S. C. Tan, *Device*, 2023, **1**, 100099.
6 X. Li, W. Xu, M. Tang, L. Zhou, B. Zhu, S. Zhu and J. Zhu, *Proc. Natl. Acad. Sci. U. S. A.*, 2016, **113**, 13953–13958.
7 X. Wang, Z. Lin, J. Gao, Z. Xu, X. Li, N. Xu, J. Li, Y. Song, H. Fu, W. Zhao, S. Wang, B. Zhu, R. Wang and J. Zhu, *Nat. Water*, 2023, **1**, 391–398.
8 N. Xu, H. Zhang, Z. Lin, J. Li, G. Liu, X. Li, W. Zhao, X. Min, P. Yao, L. Zhou, Y. Song, B. Zhu, S. Zhu and J. Zhu, *Natl. Sci. Rev.*, 2021, **8**, nwab065.
9 N. Xu, J. Li, C. Finnerty, Y. Song, L. Zhou, B. Zhu, P. Wang, B. Mi and J. Zhu, *Nat. Water*, 2023, **1**, 494–501.
10 C. Onggowarsito, A. Feng, S. Mao, L. N. Nguyen, J. Xu and Q. Fu, *ChemSusChem*, 2022, **15**, e202201543.
11 C. Onggowarsito, A. Feng, S. Mao, S. Zhang, I. Ibrahim, L. Tijing, Q. Fu and H. H. Ngo, *Environ. Funct. Mater.*, 2022, **1**, 196–203.
12 S. Mao, C. Onggowarsito, A. Feng, S. Zhang, Q. Fu and L. D. Nghiem, *J. Mater. Chem. A*, 2023, **11**, 858–867.
13 S. Mao, M. A. H. Johir, C. Onggowarsito, A. Feng, L. D. Nghiem and Q. Fu, *Mater. Adv.*, 2022, **3**, 1322–1340.
14 Y. Zhang and S. C. Tan, *Nat. Sustainability*, 2022, **5**, 554–556.
15 Y. Feng, G. Yao, J. Xu, L. Wang and G. Liu, *J. Colloid Interface Sci.*, 2023, **629**, 644–653.
16 C. Hu, W. Li, H.-Y. Zhao, C. Li, Z.-Y. Ma, L. Hao, Y. Pang, Z.-Z. Yu and X. Li, *Chem. Eng. J.*, 2023, **460**, 141622.
17 B. Yang, Z. Zhang, P. Liu, X. Fu, J. Wang, Y. Cao, R. Tang, X. Du, W. Chen, S. Li, H. Yan, Z. Li, X. Zhao, G. Qin, X.-Q. Chen and L. Zuo, *Nature*, 2023, **622**, 499–506.
18 P. Qiu, F. Liu, C. Xu, H. Chen, F. Jiang, Y. Li and Z. Guo, *J. Mater. Chem. A*, 2019, **7**, 13036–13042.
19 X.-P. Li, X. Li, H. Li, Y. Zhao, W. Li, S. Yan and Z.-Z. Yu, *Adv. Sustainable Syst.*, 2021, **5**, 2100263.
20 Y. Guo, F. Zhao, X. Zhou, Z. Chen and G. Yu, *Nano Lett.*, 2019, **19**, 2530–2536.
21 F. Yang, J. Chen, Z. Ye, D. Ding, N. V. Myung and Y. Yin, *Adv. Funct. Mater.*, 2021, **31**, 2006294.
22 J. Yan, Z. Zhang, Y. Shi, Q. Che, Q. Miao, G. Meng and Z. Liu, *New J. Chem.*, 2022, **46**, 14479–14489.

This journal is © The Royal Society of Chemistry 2024

Energy Environ. Sci., 2024, **17**, 2088–2099 | **2097**

23 T. A. Cooper, S. H. Zandavi, G. W. Ni, Y. Tsurimaki, Y. Huang, S. V. Boriskina and G. Chen, *Nat. Commun.*, 2018, **9**, 5086.

24 L. Chen, J. Ren, J. Gong, J. Qu and R. Niu, *Chem. Eng. J.*, 2023, **454**, 140383.

25 L. Li, L. Zang, S. Zhang, T. Dou, X. Han, D. Zhao, Y. Zhang, L. Sun and Y. Zhang, *J. Taiwan Inst. Chem. Eng.*, 2020, **111**, 191–197.

26 F. Wang, C. Wang, G. Shi, Y. Wang, F. Li, K. Xu and M. Ma, *Desalination*, 2023, **545**, 116157.

27 X. Xu, D. Fan, H. Zhang, J. Jing, Y. Lu and X. Yang, *Compos. Commun.*, 2023, **37**, 101438.

28 N. Cao, S. Lu, R. Yao, C. Liu, Q. Xiong, W. Qin and X. Wu, *Chem. Eng. J.*, 2020, **397**, 125522.

29 J. Ren, L. Chen, J. Gong, J. Qu and R. Niu, *Chem. Eng. J.*, 2023, **458**, 141511.

30 Y. Li, S. Zhang, Z. Xia, L. Wang and J. Fan, *Sep. Purif. Technol.*, 2023, **308**, 122852.

31 A. M. Saleque, M. N. A. S. Ivan, S. Ahmed and Y. H. Tsang, *Chem. Eng. J.*, 2023, **458**, 141430.

32 Y. Wang, X. Wu, T. Gao, Y. Lu, X. Yang, G. Y. Chen, G. Owens and H. Xu, *Nano Energy*, 2021, **79**, 105477.

33 T. Gao, Y. Wang, X. Wu, P. Wu, X. Yang, Q. Li, Z. Zhang, D. Zhang, G. Owens and H. Xu, *Sci. Bull.*, 2022, **67**, 1572–1580.

34 Y. Xu, J. Zhang, S. Wu, Y. Di, C. Liu, L. Dong, L. Yu and Z. Gan, *Energy Technol.*, 2022, **10**, 2100757.

35 Q. Zhang, X. Yang, H. Deng, Y. Zhang, J. Hu and R. Tian, *Desalination*, 2022, **526**, 115544.

36 Y. Chen, Y. Wang, J. Xu, M. R. Ibn Raihan, B. Guo, G. Yang, M. Li, H. Bao and H. Xu, *Sol. RRL*, 2022, **6**, 2200202.

37 N. Li, L. Qiao, J. He, S. Wang, L. Yu, P. Murto, X. Li and X. Xu, *Adv. Funct. Mater.*, 2021, **31**, 2008681.

38 H. Lu, W. Shi, F. Zhao, W. Zhang, P. Zhang, C. Zhao and G. Yu, *Adv. Funct. Mater.*, 2021, **31**, 2101036.

39 C. Kim, D. Shin, M. N. Baitha, Y. Ryu, A. M. Urbas, W. Park and K. Kim, *ACS Appl. Mater. Interfaces*, 2021, **13**, 29602–29611.

40 S. Zhang, Y. Deng, A. Libanori, Y. Zhou, J. Yang, T. Tat, L. Yang, W. Sun, P. Zheng, Y.-L. Zhu, J. Chen and S. C. Tan, *Adv. Mater.*, 2023, **35**, 2207916.

41 C. Li, L. Fan, R. Zhu, X. Li, P. Wen, X. Zhao, G. Wang, J. Zou and F. Kim, *ACS Appl. Energy Mater.*, 2020, **3**, 9216–9225.

42 Y. Guo, L. S. Vasconcelos, N. Manohar, J. Geng, K. P. Johnston and G. Yu, *Angew. Chem.*, 2022, **61**, e202114074.

43 X. Wei, Y. Peng, W. Fang, Z. Hu, W. Li, S. Zhang and J. Jin, *J. Mater. Chem. A*, 2022, **10**, 20424–20430.

44 Y. Guo, J. Bae, Z. Fang, P. Li, F. Zhao and G. Yu, *Chem. Rev.*, 2020, **120**, 7642–7707.

45 W. Li, X. Tian, X. Li, S. Han, C. Li, X.-Z. Zhai, Y. Kang and Z.-Z. Yu, *J. Mater. Chem. A*, 2021, **9**, 14859–14867.

46 C. Lei, W. Guan, Y. Guo, W. Shi, Y. Wang, K. P. Johnston and G. Yu, *Angew. Chem., Int. Ed.*, 2022, **61**, e202208487.

47 L. Zang, L. Sun, S. Zhang, C. Finnerty, A. Kim, J. Ma and B. Mi, *Chem. Eng. J.*, 2021, **422**, 129998.

48 F. Zhao, X. Zhou, Y. Shi, X. Qian, M. Alexander, X. Zhao, S. Mendez, R. Yang, L. Qu and G. Yu, *Nat. Nanotechnol.*, 2018, **13**, 489–495.

49 X. Zhou, F. Zhao, Y. Guo, B. Rosenberger and G. Yu, *Sci. Adv.*, 2019, **5**, eaaw5484.

50 X. Zeng, J. Yuan, W. Fang, X. He, X. Du, W. Li, L. Zhao, D. Wang and H. Chen, *Surf. Interfaces*, 2023, **43**, 103570.

51 C. Wang, J. Wang, Z. Li, K. Xu, T. Lei and W. Wang, *J. Mater. Chem. A*, 2020, **8**, 9528–9535.

52 F. Wang, Y. Su, Y. Li, D. Wei, H. Sun, Z. Zhu, W. Liang and A. Li, *ACS Appl. Energy Mater.*, 2020, **3**, 8746–8754.

53 Z. Huang, J. Wei, Y. Wan, P. Li, J. Yu, J. Dong, S. Wang, S. Li and C.-S. Lee, *Small*, 2021, **17**, 2101487.

54 H. Xing, Y. Song, H. Xu, S. Chen, K. Li, L. Dong, B. Wang, J. Xue and Y. Lu, *Small*, 2023, **19**, 2206189.

55 Y. Guo, C. M. Dundas, X. Zhou, K. P. Johnston and G. Yu, *Adv. Mater.*, 2021, **33**, 2102994.

56 S. Zhang, Y. Zhou, A. Libanori, Y. Deng, M. Liu, M. Zhou, H. Qu, X. Zhao, P. Zheng, Y.-L. Zhu, J. Chen and S. C. Tan, *Nat. Electron.*, 2023, **6**, 338–348.

57 Y. Guo, H. Lu, F. Zhao, X. Zhou, W. Shi and G. Yu, *Adv. Mater.*, 2020, **32**, 1907061.

58 X. Fan, Y. Peng, Y. Li, Y. Yang, Z. You and Y. Xu, *J. Environ. Chem. Eng.*, 2023, **11**, 110668.

59 Q. Zhang, S. Chen, Z. Fu, H. Yu and X. Quan, *Nano Energy*, 2020, **76**, 105060.

60 J. Wang, X. Cao, X. Cui, H. Wang, H. Zhang, K. Wang, X. Li, Z. Li and Y. Zhou, *Adv. Mater.*, 2024, 2311151.

61 L. Bai, H. Zhang, R. Lou, J. Li, M. Chi, J. Sha and X. Zhou, *Chem. Eng. J.*, 2023, **455**, 140934.

62 C. Li, K. Liu, H. Liu, B. Yang and X. Hu, *Mater. Res. Bull.*, 2017, **90**, 81–86.

63 E.-D. Miao, M.-Q. Ye, C.-L. Guo, L. Liang, Q. Liu and Z.-H. Rao, *Appl. Therm. Eng.*, 2019, **149**, 1255–1264.

64 J. Li, L. Yan, X. Li, W. Song and Y. Li, *J. Environ. Chem. Eng.*, 2022, **10**, 107690.

65 X. Li, G. Ni, T. Cooper, N. Xu, J. Li, L. Zhou, X. Hu, B. Zhu, P. Yao and J. Zhu, *Joule*, 2019, **3**, 1798–1803.

66 J. Zhou, Y. Gu, P. Liu, P. Wang, L. Miao, J. Liu, A. Wei, X. Mu, J. Li and J. Zhu, *Adv. Funct. Mater.*, 2019, **29**, 1903255.

67 F. Yu, Z. Chen, Z. Guo, M. S. Irshad, L. Yu, J. Qian, T. Mei and X. Wang, *ACS Sustainable Chem. Eng.*, 2020, **8**, 7139–7149.

68 K.-K. Liu, Q. Jiang, S. Tadepalli, R. Raliya, P. Biswas, R. R. Naik and S. Singamaneni, *ACS Appl. Mater. Interfaces*, 2017, **9**, 7675–7681.

69 X. Wu, L. Wu, J. Tan, G. Y. Chen, G. Owens and H. Xu, *J. Mater. Chem. A*, 2018, **6**, 12267–12274.

70 X. Wang, Z. Li, Y. Wu, H. Guo, X. Zhang, Y. Yang, H. Mu and J. Duan, *ACS Appl. Mater. Interfaces*, 2021, **13**, 10902–10915.

71 T. Li, Q. Fang, X. Xi, Y. Chen and F. Liu, *J. Mater. Chem. A*, 2019, **7**, 586–593.

72 J. Xu, S. Li, Z. Zeng and W. Xue, *J. Chem. Eng. Data*, 2019, **64**, 3793–3798.

73 B. Henderson-Sellers, *Q. J. R. Meteorol. Soc.*, 1984, **110**, 1186–1190.

74 M. Yang, H. Luo, W. Zou, Y. Liu, J. Xu, J. Guo, J. Xu and N. Zhao, *ACS Appl. Mater. Interfaces*, 2022, **14**, 24766–24774.

2098 | *Energy Environ. Sci.*, 2024, **17**, 2088–2099

This journal is © The Royal Society of Chemistry 2024

75 X. Suo, J. Yang, Y. Zhang, Y. Hao, J. Yang and H. Qiao, *Adv. Sustainable Syst.*, 2021, **5**, 2100122.

76 A. S. Alketbi, A. Raza, M. Sajjad, H. Li, F. AlMarzooqi and T. Zhang, *EcoMat*, 2022, **4**, e12157.

77 Y. Chen, H. Qiu, X. Li, Q. Tong, M. Jensen, Q. Li and N. Wang, *Appl. Surf. Sci.*, 2022, **582**, 152483.

78 Y. Shi, O. Ilic, H. A. Atwater and J. R. Greer, *Nat. Commun.*, 2021, **12**, 2797.

79 Z. Yu and P. Wu, *Adv. Mater. Technol.*, 2020, **5**, 2000065.

80 S. Vecchio, A. Catalani, V. Rossi and M. Tomassetti, *Thermochim. Acta*, 2004, **420**, 99–104.

81 Y. Tian, C. Du, S. Yong, X. Zhou, C. Zhou and S. Yang, *Chem. Eng. J.*, 2023, **453**, 139793.

82 H. W. Lim, S. H. Park and S. J. Lee, *Desalination*, 2023, **550**, 116368.

83 C. Zhang, B. Yuan, Y. Liang, L. Yang, L. Bai, H. Yang, D. Wei, W. Wang and H. Chen, *Sol. Energy Mater. Sol. Cells*, 2021, **227**, 111127.

84 J. Tang, Z. Song, X. Lu, N. Li, L. Yang, T. Sun, Y. Wang, Y. Shao, H. Liu and G. Xue, *Chem. Eng. J.*, 2022, **429**, 132089.

85 T. A. Wani, V. Gupta, P. Garg and A. Bera, *ACS Sustainable Chem. Eng.*, 2023, **11**, 9595–9600.

86 F. Wang, N. Xu, W. Zhao, L. Zhou, P. Zhu, X. Wang, B. Zhu and J. Zhu, *Joule*, 2021, **5**, 1602–1612.

87 Y. Shao, A. Shen, N. Li, L. Yang, J. Tang, H. Zhi, D. Wang and G. Xue, *ACS Appl. Mater. Interfaces*, 2022, **14**, 30324–30331.

88 L. Yang, T. Sun, J. Tang, Y. Shao, N. Li, A. Shen, J. Chen, Y. Zhang, H. Liu and G. Xue, *Nano Energy*, 2021, **87**, 106163.

89 W. Wang, Y. Shi, C. Zhang, S. Hong, L. Shi, J. Chang, R. Li, Y. Jin, C. Ong, S. Zhuo and P. Wang, *Nat. Commun.*, 2019, **10**, 3012.

90 E. Chiavazzo, M. Morciano, F. Viglino, M. Fasano and P. Asinari, *Nat. Sustainability*, 2018, **1**, 763–772.

91 L. Huang, H. Jiang, Y. Wang, Z. Ouyang, W. Wang, B. Yang, H. Liu and X. Hu, *Desalination*, 2020, **477**, 114260.

92 X. Li, W. Xie and J. Zhu, *Adv. Sci.*, 2022, **9**, 2104181.

93 X. Gu, K. Dong, L. Peng, L. Bian, Q. Sun, W. Luo and B. Zhang, *Energy Convers. Manage.*, 2023, **277**, 116634.

94 S. Zhao, X. Zhang, G. Wei and Z. Su, *Chem. Eng. J.*, 2023, **458**, 141520.

95 R. Peeters, H. Vanderschaeghe, J. Rongé and J. A. Martens, *iScience*, 2021, **24**, 103266.

96 H.-J. Li, L. Cheng, P. Sun, F.-F. Li and J. Qiu, *Water*, 2023, **15**, 878.

This journal is © The Royal Society of Chemistry 2024

Energy Environ. Sci., 2024, **17**, 2088–2099 | **2099**